Observation of a frequency-dependent doublet in the Si-B3 ESR spectrum

2010 J. Phys.: Condens. Matter 22 095801

(http://iopscience.iop.org/0953-8984/22/9/095801)

J. Phys.: Condens. Matter **22** (2010) 095801 (5pp) doi:10.1088/0953-8984/22/9/095801

Observation of a frequency-dependent doublet in the Si-B3 ESR spectrum

K Keunen[1] **and A Stesmans**

Department of Physics, University of Leuven, Celestijnenlaan 200D, B-3001 Leuven, Belgium
and
INPAC—Institute for Nanoscale Physics and Chemistry, University of Leuven,
B-3001 Leuven, Belgium

E-mail: koen.keunen@fys.kuleuven.be

Received 3 September 2009, in final form 18 November 2009
Published 10 February 2010
Online at stacks.iop.org/JPhysCM/22/095801

Abstract
The Si-B3 spectrum, observed in neutron-irradiated p-type silicon after annealing at $T_{an} \approx 400\,^{\circ}C$, has previously been extensively studied using electron spin resonance (ESR). It has been assigned to a silicon tetra-interstitial (I_4), based on the symmetry of the defect and resolved hyperfine (hf) structure doublets. However, additional ESR measurements carried out here at three frequency bands show that one of these doublets would not originate from the hf interaction since the doublet spacing is found to be dependent on the applied microwave frequency f. This casts doubt on the previous assignment of the Si-B3 spectrum to I_4 based on ESR data obtained at one observational f. Despite profound investigation, the origin of the f dependence of the satellite doublet could not be traced, disabling any progress on the Si-B3 defect modeling. The observation (re)emphasizes the necessity of the multi-frequency approach in coming to a correct interpretation of ESR parameters and correlated defect modeling.

1. Introduction

In semiconductors, such as Si, it is widely accepted that self-interstitials play an important role in various dynamic phenomena such as self-diffusion [1] and the transient enhanced diffusion of dopant impurity atoms [2–4] (such as boron) during thermal processing, causing a broadening of diffusion profiles and dopant deactivation [5], thus possibly limiting the downscaling of next-generation submicron semiconductor devices. It is therefore important to gain an understanding of the atomic nature of the interstitial-like defects. Electron spin resonance (ESR) has proven to be the tool of choice for the atomic identification of point defects and its use has enabled reliable identification of various types of defects in Si [6]. In this, hyperfine (hf) interaction and resolved anisotropy are the dominant elements in providing a trustworthy model of the defect since the hf interaction provides information about the atomic surroundings of the unpaired electron, such as the identification of the surrounding atoms, number of equivalent atoms in a shell, the localization of the resonant electron on each shell and s–p hybridization ratio of the unpaired orbital over the different atom sites. For defects in non-isotopically enriched Si, however, resolving and full angular mapping of hf structure is often inaccessible, as the natural abundance of ^{29}Si (nuclear spin $I = 1/2$) is only 4.67%.

As to small interstitial clusters in Si, defect identification backed up by theory still appears limited. A single interstitial positioned at a tetrahedral site has been tentatively proposed as the defect model of the AA12 ESR spectrum [7] while the Si-P6 spectrum has been linked to a di-interstitial configuration with C_2 symmetry [8]. Yet, recent calculations indicate that the proposed structure is metastable and I_2 would exhibit C_{1h} symmetry at low temperatures [9, 10], leaving the true nature of the Si-P6 spectrum still unclarified.

The present work deals with the Si-B3 spectrum, which has been assigned to the Si tetra-interstitial (I_4) based on several experimental [11, 12] and theoretical [13] reports. Both experimental works reported the observation of three resolved doublets of hf interaction which formed the basis of the assignment of the Si-B3 to the I_4. However, as will be shown below, the spacing of one of these doublets appears dependent on the observational ESR microwave frequency f, casting doubts on the hf origin of this doublet. This, as a consequence, raises questions about the assignment of the Si-B3 to the tetra-interstitial. Unfortunately, we fail to explain this f dependence and, as such, cannot come to grips with

[1] Author to whom any correspondence should be addressed.

Table 1. Comparison of the inferred hyperfine structure parameters for the Si-B3 spectrum between different ESR works.

	Reference [11] [a]			Reference [12] [b]		
Shell number	No. equiv. Si atoms	$A_{\parallel}$ (G)	$A_{\perp}$ (G)	No. equiv. Si atoms	$A_{\parallel}$(G) $\pm$ 0.2	$A_{\perp}$(G) $\pm$ 0.2
I	2	13.9	4.5	2	13.6	7.6
II	8	5.2	3.2	4	5.4	5
III	12	2.7	1.9	8	2.9	2.2

[a] 9.0 GHz data. [b] 20.5 GHz data.

improvement in defect modeling, let alone proposing a new defect model. Rather, this paper is intended to stress the importance of measuring at different frequency bands in order to correctly interpret ESR parameters and come to reliable defect modeling—a practice often neglected.

2. ESR work on Si-B3

The Si-B3 spectrum was first reported in 1970 by Daly [14] in boron-doped (2×10^{17} B cm^{-3}) silicon after irradiation with 6.6×10^{15} neutrons cm^{-2} and subsequent annealing at 270 °C for 20 min. The Si-B3 spectrum exhibits an unusual tetragonal D_{2d} symmetry with principal g matrix values given by $g_{\parallel}(\parallel[100]) = 2.0161 \pm 0.0001$ and $g_{\perp} = 2.0052 \pm 0.0001$. A thorough ESR investigation, including experiments under applied mechanical stress, performed later by Brower [15] showed the inferred D_{2d} symmetry to be inherent, i.e. not related to Jahn–Teller distortion. Brower also argued, based on group theory and a knowledge of vacancy centers, the defect to be intrinsic and of the interstitial type rather than related to vacancy clusters. Due to a lack of detailed hf information, however, the true nature of the Si-B3 defect could not be assigned unambiguously and the (100) di-interstitial and split interstitial were tentatively proposed as possible defect models. In 2003, Mchedlidze and Suezawa [11] and Pierreux and Stesmans [12] reported on a detailed ESR analysis of the Si-B3 spectrum, with both groups being able to resolve up to three hf doublets, indicating the interaction of the defect's unpaired electron with at least three shells of equivalent Si atoms.

Mchedlidze and Suezawa [11] performed X-band measurements on annealed p-type Si samples, irradiated at room temperature with 4×10^{17} electrons cm^{-2}. Subsequent annealing of the samples was carried out in an Ar flow at 400 °C for 5 h. The measured spectra were decomposed in several components, i.e. individual peaks with Gaussian lineshape and the same line width, corresponding to the central Zeeman line and the three hf doublets. Best fitting results were obtained using a first shell containing two equivalent Si atoms, a second shell comprised of eight equivalent Si atoms and a third containing twelve equivalent Si atoms (from here on denoted as a set of 2–8–12 equivalent Si atoms). It should be mentioned, however, that no second-order interaction or intershell interaction (i.e. the interaction of the defect's unpaired electron with multiple ^{29}Si atoms in the three shells of equivalent Si sites) was taken into account in these fittings.

Pierreux and Stesmans [12] carried out K-band measurements on p-type (10^{17} B cm^{-3}) (100) Si samples, which were irradiated by high-energy neutrons ($\sim 10^{18}$ cm^{-2}) and subsequently annealed in the range 350–450 °C for about 40 min. Here the measured spectra were analyzed using a computer code based on the simplified spin Hamiltonian, taking into account the full second-order and intershell interaction, thus in essence providing a more reliable fitting. Best fitting results were obtained when using a set of 2–4–8 equivalent Si atoms—two equivalent Si atoms in a first shell, four equivalent Si atoms in a second shell and eight equivalent Si atoms in a third shell.

The principal hf tensor values, extracted from the fitting procedures by the two groups, are given in table 1. It is clear that, while both discuss the same Si-B3 spectrum, the results, concerning the number of equivalent Si atoms in an interacting shell and the principal hf tensor values, are not equal. It should be noted, however, that analysis of hf structure is an intricate procedure for the following two reasons: (1) the natural abundance of ^{29}Si (only 4.67%) makes the correct determination of the relative intensity of hf doublets to the main Zeeman line difficult and (2) there is the presence of obscuring and overlapping foreign signals not belonging to the Si-B3 spectrum, hampering the full angular mapping of the hf structure. Yet, inspired by theory [13], both research groups proposed the tetra-interstitial as the defect model for the Si-B3 based on the tetragonal symmetry and the newly resolved hf information. Since, and despite the differences in the reported set of equivalent Si sites and principal hf tensor values, the assignment of I_4 to the Si-B3 spectrum has been considered rather definite.

Considering the difficulties encountered when analyzing the intensity of hf doublets and principal hf tensor values, we will not attempt here to determine which of the two sets, if any, of equivalent Si atoms is the correct one. Instead, this work will deal with an uncommon and rather disturbing behavior of one of the resolved doublets, which has been assumed to arise from hf interaction. Very surprisingly, and unlike the other hf structure, the splitting of the second doublet (cf doublet II in table 1) is found to depend on the frequency, indicating that it may not originate from ^{29}Si hf interaction at all, possibly raising serious doubts about the assignment of I_4 as a defect model for the Si-B3 spectrum. Furthermore, this observation stresses the importance of measuring ESR at multiple frequencies in order to make unambiguous interpretation of measured spectral features, required for conclusive assignment of the atomic defect model.

3. Experimental details

The samples studied were slices of the 2×9 mm^2 main face, cut from B-doped (10^{17} cm^{-3}) (100)Si wafers about 500 μm

thick, with the 9 mm edge along the $[0\bar{1}1]$ direction. These were irradiated by high-energy neutrons (peak energy 3 MeV; 10^{18} cm^{-2}) and subsequently annealed at $T_{an} = 400\,^{\circ}$C for $\approx$40 min. This temperature was previously determined as the optimal T_{an} for the Si-B3 with respect to signal intensity and selective out-annealing of interfering signals, which would otherwise obfuscate the analysis of hf information. The ESR measurements were carried out at around 40 K employing X- ($\sim$8.9 GHz), K- ($\sim$20.5 GHz) or Q-band ($\sim$33.5 GHz) spectrometers driven in the adiabatic slow passage mode, as described elsewhere [16, 17], with the applied magnetic field **B**, at an angle φ_B to the sample normal **n**($\|$[100]), rotating in the $(0\bar{1}1)$ plane. The g values were determined using a comounted Si:P marker sample. Special care was exercised to keep the incident microwave power P_μ and the amplitude B_m of the sinusoidal modulation ($\approx$0.2 G, typically at $\approx$100 kHz) of the applied magnetic field appropriately limited so as to record undistorted signals.

4. Experimental results and analysis

As outlined previously [12], the Si-B3 spectrum can be described by the simplified spin Hamiltonian composed of the electronic Zeeman interaction and the hf interaction terms:

$$H = \beta \mathbf{B} \cdot \hat{g} \cdot \mathbf{S} + \sum_j \mathbf{I}_j \cdot \hat{A}_j \cdot \mathbf{S}, \qquad (1)$$

with effective electronic spin $S = 1/2$. Here, β represents the Bohr magneton, $\hat{g}$ is the electronic g dyadic and $\hat{A}_j$ is the hf tensor for the interaction of the electronic spin with the jth group of equivalent lattice sites. We interpret the hf structure as arising solely from interaction with ^{29}Si nuclei (4.67% abundant, $I = 1/2$). Spectral analysis was carried out using a computer code involving exact matrix diagonalization and based on equation (1), complemented on the right-hand side with the nuclear Zeeman term $\sum_j g_N \beta_N \mathbf{B} \cdot \mathbf{I}_j$ to take into account second-order (Breit–Rabi) corrections. Here, g_N and β_N represent the nuclear g factor and magneton, respectively. This code was used to simulate the measured Si-B3 spectra in order to determine the hf parameters, such as hf splitting and the number of equivalent interacting sites in each shell. Special care was taken to convincingly reproduce the various hf spectral features, including 'second-order' structure (resulting from multiple site occupation by ^{29}Si nuclei and intershell interaction).

The Si-B3 resonance is found to show some slight asymmetry, clearly exposed by the central Zeeman signal, as was reported by Pierreux and Stesmans [12]. It was ascertained that this asymmetry did not result from a measurement artifact by thoroughly checking the influence of relevant experimental parameters such as the incident microwave power, modulation field amplitude, observational temperature, and sweep rate and width. Since the asymmetry seems to be inherent, the simulations were performed by the introduction of a (slight) asymmetric distribution ($\leqslant$0.1%) on the g value as the line broadening mechanism.

Figure 1 shows zoomed-in parts of typical K-band ESR spectra, observed at 40 K for two orientations of **B**, together

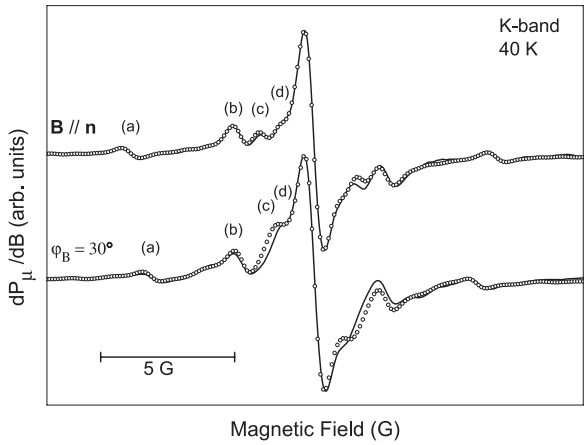

Figure 1. Zoomed-in parts of experimental K-band first-derivative absorption ESR spectra of the Si-B3 defect (full curves) centered on the low magnetic field signal for two orientations of the applied magnetic field. Open circles correspond to optimized computer simulations based on the interaction with one shell of two equivalent Si atoms (doublet (a)) and three shells of six equivalent Si atoms each (doublets (b)–(d)).

with computer simulations (open circles). The spectral region shown represents extended views of the low field Zeeman signal, this region being the least perturbed by interfering signals originating from other defects. The Si-B3 spectra observed for **B** $\|$ **n** clearly show four first-order hf doublets, labeled (a)–(d) in decreasing order of hf splitting. For most values of φ_B, however, the limited field separation between the doublet (c) and (d) signals makes it hard to distinguish these two doublets. The simulations shown correspond to a set of 2–6–6–6 equivalent Si atoms for doublets (a)–(b)–(c)–(d), respectively. It turned out to be difficult to select one set of shells of equivalent Si atoms that could globally enable optimal simulation of all K-band spectra taken for different orientations of **B**. While not generally perfect, this set resulted in the best overall fitting over the results obtained at the three microwave frequencies of the resolved ^{29}Si hf structure—somewhat more satisfactory than with the 2–4–8 set previously inferred basically on single f ESR data. However, as mentioned before we will not enter further into this.

A more disturbing feature shows up when we compare the measurements at the three different frequencies. Figure 2 presents spectra measured at 40 K with **B** $\|$ **n** together with computer simulations (open circles) for three ESR frequencies. The simulations shown were carried out using a set of 2–6–6–6 equivalent Si atoms, the same set as used (see above) to simulate the K-band spectra, which gives satisfactory results for the X- and Q-band spectra as well. For the doublets (a), (c) and (d) the same hf splitting values could be used in all three frequency bands, showing these to be independent (in first order) of observational frequency, as one would expect from doublets arising from the hf interaction. For doublet (b), however, it was not possible to use one such hf splitting value for the three frequencies. It can be clearly seen in figure 2 that, while the field splitting (position) of doublets (a), (c) and (d) remains fixed, the position of doublet (b) changes over the three f bands, the splitting as fitted varying from

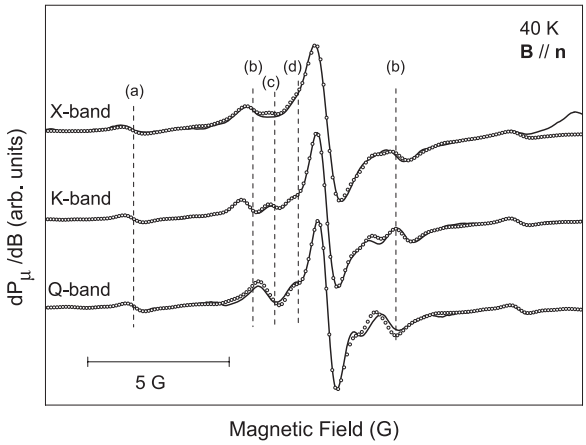

Figure 2. Comparison of experimental X-, K- and Q-band ESR spectra of the Si-B3 defect (full lines), observed at 40 K with the applied magnetic field along the (100) normal. Computer simulations (open circles) correspond to interaction with a set of 2–6–6–6 equivalent Si atoms for doublets (a)–(b)–(c)–(d), respectively. The dashed lines, meant to guide the eye, clearly expose the frequency dependence of doublet (b).

5.1 ± 0.2 G in the X-band over 5.4 ± 0.2 G in the K-band to 4.5 ± 0.2 G in the Q-band. Again, this feature was thoroughly tested not to concern an artifact of measurement by checking all possible measurement parameters such as field sweep rate and width, lock-in time constant, B_m, P_μ and T. It is also worth mentioning that, unexpectedly, the peak-to-peak linewidth of the Si-B3 resonance decreases from $\Delta B_{\rm pp} = 0.90$ G in the X-band to $\Delta B_{\rm pp} = 0.65$ G in the Q-band. This is accompanied by a noticeable decrease in the asymmetry of the resonance line with increasing f.

5. Interpretation and discussion

The uncovered f dependence of the doublet (b) hf splitting raises serious doubts as to the real ^{29}Si origin of these satellite lines. They cannot result from the usual hf interaction, including interaction with an H atom, since the separation of the hf satellites should be independent of f to first order (neglecting the Breit–Rabi interaction, which is marginal for the kind of small splittings as encountered here [18]). So, in a first categorical reaction, one may simply put forward this doublet (b) not to be part of the Si-B3 spectrum at all, perhaps not even concerning a hf structure. This would really threaten the previous assignment to the I_4 indeed.

Evidently, though, the satellite lines (b) clearly cannot arise from other defects of different g values since the separation of such lines would scale down proportionally with decreasing f, unlike observations. An impurity-related origin is thus ruled out as well. Furthermore, the satellites are perfectly centered at the g value of the central Zeeman signal for both branches of the Si-B3 spectrum and for all orientations of **B**, the different observational temperatures and the three ESR frequencies used, asserting that these satellites belong to the Si-B3 spectrum. It seems to raise a dilemma.

Next, in an attempt to trace the origin of the satellite lines, the literature was searched for reports on f-dependent behavior of satellite lines. Holder *et al* [19] reported on a f-dependent spacing of satellite lines observed in diamond films grown by chemical vapor deposition (CVD), with the spacing varying from 5.6 G at the X-band to 17.5 G at the Q-band. They explained this behavior by taking into account the dipole–dipole interaction between the resonant electron and a nearby proton. The resulting forbidden electron–proton spin flip satellites should be separated by $\delta B = g_{\rm N}\beta_{\rm N}B_{\rm a}/g_{\rm e}\beta$, as worked out by Trammel *et al* [20], where $g_{\rm N}$ and $g_{\rm e}$ are the nuclear and free electron g factor, respectively, and $B_{\rm a}$ is the average resonant field of the two satellite lines. The spacing of the satellite lines would thus be proportional to the applied f and the theory furthermore predicts the ratio of the amplitudes of the satellite lines relative to the central Zeeman line to reduce at higher frequencies with a factor of at least $1/f^2$. However, neither the separation nor the observed intensity of the satellite lines (b) in figure 2 matches these predicted tendencies.

Another f dependence of satellite spacing of a defect spectrum was observed in CVD diamond by Talbot-Ponsonby *et al* [21], with the separation increasing from around 9.7 G at 3.5 GHz to 12.5 G at 9.5 GHz. The relation of the satellite spacing to f does not match the model described above, where the unpaired electron would interact with a weakly coupled nucleus. Instead, the satellites are proposed to originate from a pair of coupled electron spins which form a biradical center. Under the assumption that the coupling between the two spins is only due to isotropic exchange, the separation between the satellite lines was calculated as

$$\delta B = \frac{[J^2 + (g_a - g_b)^2\beta^2B^2]^{1/2} + J}{\frac{1}{2}(g_a + g_b)\beta}, \qquad (2)$$

where g_a and g_b are the unpaired electron g values and J is the isotropic exchange coupling constant between the two spins. Again, however, the relationship between the satellite spacing and f predicted by this model does not correspond to the observed spacing of doublet (b) in figure 2, as in this model the satellite spacing should increase monotonically with enhancing f.

So, despite perusal of previous experimental and theoretical work, no explanation can be offered for the observed f-dependent behavior of the satellite lines (b). No similar previous observation could be traced.

6. Concluding remarks

A multi-frequency ESR analysis has been carried out of the prominent tetragonal Si-B3 spectrum in n-irradiated Si with the intention to enhance reliability of the previous assignment to the I_4 defect through providing a broader experimental footing. According to standard practice, this was focused on resolving experimentally a detailed and correct spectral hf structure at three ESR frequencies, for various observational parameters, which, globally, should be amenable to consistent simulation by one set of spin Hamiltonian ESR parameters, culminating in high reliability. This, however, turns out differently.

Optimized ESR spectroscopy has enabled us to resolve four principal doublets as ^{29}Si hf structure, which has been studied in detail as a function of various pertinent experimental

parameters. Unlike the major part of the ^{29}Si hf structure, one hf doublet was found to exhibit a remarkable f dependence, in that the separation of the two lines is increasing from the X-band to K-band to decrease again for the Q-band to a splitting even smaller than the X-band one. Other unexpected observations include that the linewidth as well as the inherent asymmetry of the Si-B3 resonance is decreasing with increasing f. It was repeatedly tested that these features did not result from measurement artifacts and the spectra could be well reproduced in all three frequency bands. These observations raise uncertainty about the assignment of the Si-B3 spectra to the tetra-interstitial defect, whose modeling should thus be treated critically, and heavily stress the importance of multi-frequency ESR measurements.

Best fitting over all three ESR frequency data is attained using a 2–6–6–6 set of shells of equivalent Si sites, the previously inferred set of 2–4–8 appearing less satisfying. While it could be ascertained that the f-dependent hf doublet is part of the Si-B3 hf structure, no obvious explanation could be offered as to its behavior. So, the current results fail to add to enhanced confidence in defect modeling. Rather, as a major result, the current work strongly emphasizes the combination of multi-frequency ESR probing as a mandatory aspect in order to come to reliable defect identification.

References

[1] Blöchl P E, Smargiassi E, Car R, Laks D B, Andreoni W and Pantelides S T 1993 *Phys. Rev. Lett.* **70** 2435

[2] Cowern N E B, Godfrey D J and Sykes D E 1986 *Appl. Phys. Lett.* **49** 1711

[3] Kohyama M and Takeda S 1992 *Phys. Rev.* B **46** 12305

[4] Eaglesham D J, Stolk P A, Gossmann H J and Poate J M 1994 *Appl. Phys. Lett.* **65** 2305

[5] Stolk P A, Grossmann H J, Eaglesham D J, Jacobson D C, Rafferty C S, Gilmer G H, Jaraiz M, Poate J M, Luftman H S and Haynes T E 1997 *J. Appl. Phys.* **81** 6031

[6] See, e.g., Watkins G D 2000 *Mater. Sci. Semicond. Process.* **3** 227 and references therein

[7] Mukashev B N, Abdullan K A and Gorelkinskii Y V 1998 *Phys. Status Solidi* a **168** 73

[8] Lee Y H, Gerasimenko N N and Corbett J W 1976 *Phys. Rev.* B **14** 4506

[9] Kim J, Kirchoff F, Aulbur W G, Wilkins J W, Khan F S and Kresse G 1999 *Phys. Rev. Lett.* **83** 1990

[10] Jones R, Eberlein T A G, Pinho N, Coomer B J, Goss J P, Briddon P R and Berg S 2002 *Nucl. Instrum. Methods Phys. Res.* B **186** 10

[11] Mchedlidze T and Suezawa M 2003 *J. Phys.: Condens. Matter* **15** 3683

[12] Pierreux D and Stesmans A 2003 *Phys. Rev.* B **68** 193208

[13] Coomer B J, Goss J P, Jones R, Öberg S and Briddon P R 2001 *J. Phys.: Condens. Matter* **13** L1

[14] Daly D F 1971 *J. Appl. Phys.* **42** 864

[15] Brower K L 1976 *Phys. Rev.* B **14** 872

[16] Van Gorp G and Stesmans A 1992 *Phys. Rev.* B **45** 4344

[17] Stesmans A, Nouwen B and Iakoubovskii K 2000 *J. Phys.: Condens. Matter* **12** 7807

[18] See, e.g., Weil J A, Bolton J R and Wertz J E 1994 *Electron Paramagnetic Resonance: Elementary Theory and Practical Applications* (New York: Wiley) p 116

[19] Holder S L, Rowan L G and Krebs J J 1994 *Appl. Phys. Lett.* **64** 1091

[20] Trammel G T, Zeldes H and Livingston R 1958 *Phys. Rev.* **110** 630

[21] Talbot-Ponsonby D F, Newton M E, Baker J M, Scarsbrook G A, Sussmann R S and Wort C J H 1996 *J. Phys.: Condens. Matter* **8** 837